EUROPEAN FUSION DEVELOPMENT AGREEMENT

EFDA–JET–PR(03)46

M-L Mayoral, D.N. Borba, R. Buttery, S. Coda, L.-G. Eriksson, T.T.C. Jones,
V. Kiptily, M.J. Mantsinen, A. Mück, J.-M. Noterdaeme, S.D. Pinches,
O. Sauter, S. Sharapov and JET EFDA contributors

Studies of Burning Plasma Physics in the Joint European Torus

Studies of Burning Plasma Physics in the Joint European Torus

M-L Mayoral[1], D.N. Borba[5], R. Buttery[1], S. Coda[3], L.-G. Eriksson[4], T.T.C. Jones[1], V. Kiptily[1], M.J. Mantsinen[2], A. Mück[6], J.-M. Noterdaeme[6,7], S.D. Pinches[6], O. Sauter[3], S. Sharapov[1] and JET EFDA contributors*

[1]EURATOM/UKAEA Fusion Association, Culham Science Centre, Abingdon,OX14 3DB, UK
[2]Helsinki University of Technology, Association Euratom-Tekes, Finland
[3]Centre de Recherches en Physique des Plasmas, EPFL, Association Euratom Confédération Suisse, Lausanne, Switzerland
[4]Commissariat à l'Energie Atomique de Cadarache, Association EURATOM/CEA, Saint-Paul-Lez-Durance, France
[5]Centro de Fusão Nuclear/IST, Lisbon, Portugal
[6]Max-Planck-Institut für Plasmaphysik- EURATOM Assoziation, Boltzmann-Str2, D 85748, Garching, Germany
[7]Max-Planck-Institut für Plasmaphysik-EURATOM Assoziation, Boltzmann-Str2, D-85748, Garching, Germany and Gent University, Department EESA, Belgium
**See annex of J. Pamela et al, "Overview of Recent JET Results and Future Perspectives", Fusion Energy 2000 (Proc. 18th Int. Conf. Sorrento, 2000), IAEA, Vienna (2001).*

Preprint of Paper to be submitted for publication in
Physics of Plasma

‘‘This document is intended for publication in the open literature. It is made available on the understanding that it may not be further circulated and extracts or references may not be published prior to publication of the original when applicable, or without the consent of the Publications Officer, EFDA, Culham Science Centre, Abingdon, Oxon, OX14 3DB, UK.”

“Enquiries about Copyright and reproduction should be addressed to the Publications Officer, EFDA, Culham Science Centre, Abingdon, Oxon, OX14 3DB, UK.”

ABSTRACT

In burning plasma experiments, the very energetic alpha (α) particles resulting from deuterium-tritium fusion reaction will be the dominant heating mechanism and will give rise to new physics issues. Recent experiments performed on the Joint European Torus (JET) [P.H. Rebut and B.E. Keen, Fusion Technology **11**, 13 (1987)] and aiming to investigate burning plasma physics, are reported in this paper. In the presence of very energetic particles, the magneto-hydrodynamic (MHD) stability of plasmas is affected. Sawteeth will be strongly stabilised and may lead to the onset of Neo-classical Tearing Modes (NTMs), which are damaging for the plasma confinement. ^{4}He ions injected at 120keV by the Neutral Beam Injection system (NBI) and accelerated by Ion Cyclotron Resonance Frequency (ICRF) waves to the MeV energy range have provided the necessary energetic particles to investigate these effects. New scenarios have been used in order to control the stability of the sawteeth even in the presence of fast particles and to prevent or delay the appearance of NTMs. Finally, in a plasma self-heated by a-particles, the thermal stability is a critical point and a equilibrium will have to be maintained between the a-heating and the transport losses. Experiments have been performed where a fraction of the ICRF heating has been used to simulate the a-heating. A situation of thermal runaway has been demonstrated and successfully controlled.

I. INTRODUCTION

In magnetic fusion, the reaction with the highest cross section at the lowest plasma temperature, is the one in which the nuclei of deuterium and tritium fuse to produce an alpha (α) particle (i.e. 3.5MeV ^{4}He ions) with the release of a neutron, that is: ${}^{2}_{1}D + {}^{3}_{1}T \rightarrow {}^{4}_{1}He\ (3.5MeV + {}^{1}_{0}n\ (14.1MeV)$. Four fifths of the reaction energy is then carried by the neutrons which leave the plasma without interaction and the remainder by the a-particles which will transfer their energy mostly to thermal electrons which in turn heat the plasma ions through collisions. Once enough fusion reactions take place and if the confinement is sufficiently good, the fusion energy production overcomes the plasma energy loss by such mechanism as radiation and the reaction becomes self-sustained. A measure of fusion performance is the fusion gain factor, Q, defined as the ratio of the fusion power produced P_{fusion} over the input power to the plasma *ext* P_{ext}: $Q = P_{fusion} / P_{ext}$. Another criterion of relevance is the fraction of a-heating to the total power, f_α defined as $f_\alpha = Q / Q + 5)$. Given the trade-off between power generation efficiency and controllability of the plasma, it is foreseen that fusion reactors will operate in the range Q ~ 30-50, which corresponds to a fraction of α-heating of 85 to 90%. This defines the target of the "burning plasma". The main goal of the International Thermonuclear Energy Reactor (ITER) [1] is to achieve an "extended burn" i.e. Q ≥ 10 for ~300 to 500s, longer than the characteristic time scales of plasma processes, with α-heating corresponding to around two third of the total heating power. The physics program of ITER burning plasmas will include of two key studies:

- Energetic particles physics: The main properties of energetic particles like the 3.5MeV α-particles are centrally peaked profiles, heating of electrons and characteristic velocity exceeding

the Alfvén velocity of the thermal plasma. In particular, because of their peaked pressure gradient, these super-alfvénic particles are capable of interacting with global MHD waves known as Alfvén eigenmodes (AEs)[2]. Depending on their spatial distribution, energetic particles can also either stabilise $m = 1$, $n = 1$ modes (where m and n are the poloidal and toroidal modes numbers respectively), leading to the monster sawtooth phenomenology observed on JET [3,4,5] or destabilise fishbone modes [6].

- Self-heating and thermal stability: Controlled, steady state operation of a burning plasma implies that transport power losses balances the sum of the self-heating from the α-particles and the external heating power. A thermally stable solution further requires that the transport losses increase more rapidly with temperature than the sum of the fusion power and external power, assuming a feedback loop that decreases the external power as the a-particles heating increases. In the case of a sudden change in the confinement mode or the creation of a transport barrier for the particles and heat, the transport power losses, thus the thermal equilibrium, will be strongly affected. In order to study the plasma thermal stability for different operating regimes in present tokamaks, experiments simulating a burn control can be conceived using feedback from measurements of the temperature or neutron rate to control the heating power.

In order to progress in the burning plasma physics issues, the JET tokamak has several unique capabilities. First of all, because of the large physical size of the machine and high plasma current capabilities (up4 MA), MeV ions orbit widths are small compared to the plasma minor radius leading to well confined very energetic ions. JET also has on one hand a powerful Ion Cyclotron Resonance Frequency (ICRF) system capable of accelerating ions to MeV energy and on the other hand a Neutral Beam Injection (NBI) system capable of long pulse operation with a large range of beam ions: D, H, ^{3}He, T and ^{4}He. Moreover, JET has a very complete set of diagnostics. Among them, coils for excitation and detection of stable AEs, gamma ray (γ-ray) spectroscopy, neutron and neutral particle analyser diagnostics, which are of critical importance for burning plasma studies. Finally, the possibility to operate with D-T plasmas is also of great relevance for burning plasma studies.

In this paper we present four sets of experiments related to burning plasma physics studies and recently performed on JET. First we describe experiments in which ^{4}He beam ions have been accelerated to MeV energies using ICRF heating at the 3rd harmonic of the ^{4}He cyclotron resonance. The presence of such high energetic particles was confirmed by γ-ray emission and by the presence of elliptical and toroidal Alfvén eigenmodes (EAEs and TAEs).

In the second part, we concentrate on the control of sawtooth activity. Indeed, fast particlesstabilised sawtooth can lead to the onset of neoclassical tearing modes (NTMs) for normalised plasma pressure β_N much lower than the target requirement for ITER, where $\beta_N = \beta(\%)/[I_p\,(MA)/a(m)B\mathrm{T}]$, $\beta = \langle p \rangle /(B^2/2\mu_0)$, p is the plasma pressure, B is the magnetic field at the plasma centre, I_p is the plasma current and a is the plasma minor radius. Since these modes have a very

detrimental effect on the plasma performance we study the possibility to control the sawtooth activity and thus the NTMs onset by using Ion Cyclotron Current Drive (ICCD).

Finally, we present experiments aiming to simulate the a-particles self-heating. In particular, we demonstrate the possibility of thermal runaway for a simulated 10 = Q equivalent burn and its control by feedback on the external power.

2. ALPHA-TAIL PRODUCTION WITH ION CYCLOTRON RESONANCE HEATING OF ^{4}HE-BEAMS IONS

Experiments in ^{4}He plasmas on JET have been carried out in order to produce MeV-energy ^{4}He ions accelerated by ICRF heating [7]. By working with a magnetic field B of 2.2T and an ICRF wave frequency $f = \omega(2\pi)$ of 51 MHz, the third harmonic ^{4}He ion cyclotron resonance, $\omega \approx \omega_c\ ^4He$, was positioned in the plasma centre. Up to 8MW of ICRF power, P_{ICRF}, was applied with a symmetric toroidal mode spectrum (dipole phasing).

For high-harmonic ICRF scenarios such as $\omega \approx 3\omega_c$ (^4He), the ICRF wave absorption by the resonating ions increases with ratio of the ion Larmor radius ρ to the perpendicular wavelength of the fast wave until a maximum is reached, which typically occurs at ion energies in the MeV range. In order to ensure significant third harmonic absorption, ^{4}He fast neutrals from NBI with energy E_b in the range of 70 - 120keV and ρ in the range of 1.4 - 2.2cm, were added to plasmas heated by ICRF power. A relatively low NBI power of about 2.2MW was found effective in creating a sufficient number of ^{4}He ions with high enough ρ to be accelerated to high energies by ICRF waves. As illustrated in Figure 1 clear differences in the global plasma characteristics were observed as the beam energy E_b was increased from 70 to 120keV, which increased the ^{4}He single-pass damping. The total stored plasma energy W_{DIA} and the electron temperature T_e (at a normalised minor radius $r/a \approx 25$) were significantly higher with 120 than with 70keV beam.

Information on confined ^{4}He ions was obtained with the g-ray spectrometer [8] for the discharges shown in Figure 1. The peaks in the measured γ-ray energy spectra (Figure 2) at γ energy of 4.4 MeV are due to g emission from the nuclear reaction ^{9}Be(α, $n\gamma$)^{12}C between ICRF-accelerated ^{4}He ions and intrinsic beryllium impurity ions present in JET plasmas. This reaction cross-section depending on the α-particle energy (with a resonance at $E_\alpha \approx 2$MeV and a number of resonance at $E_\alpha \geq 4$MeV) was previously proposed as a diagnostic for fusion-born a-particles 9, and has been successfully tested for the first time during this set of experiments. The analysis of the spectra shows that when the beam energy was increased from 70 keV to 120 keV, the number of a-particles with an energy greater than 2MeV increased by a factor of 5. It has to be noted that without beams, as that no ^{4}He with energy above 2MeV were produced, no peaks at the γ-ray energy of 4.4 MeV were observed.

The electron temperature T_e was found to increase with the fast particles energy content W_{fast} (with $W_{fast} = 2)W_{fast} - W_{th}$) / 3 and W_{th} the thermal stored plasma energy deduced from measured plasma densities and temperatures), indicating effective power transfer from fast ^{4}He to electrons.

It has been estimated that, in the discharge 54165 represented on Figure 1, fast ^{4}He ions provided about 80%-90% of the total heating power to the thermal plasma [7].

Important information on the fast ion distribution was provided by the AEs activity, which is a good indicator 10,11 of the presence of high-energy ions with velocities comparable to or greater than the Alfvén speed in the plasma. Magnetic fluctuation spectrograms measured using an array of Mirnov coils at the plasma edge [12,13] show $|\delta B/\delta t|$ versus time and frequency, in the frequency range of 0 to 500kHz. In Figure 3, for the discharges with 120keV beams, the activities in the 150-200kHz range and 370-420kHz range can be identified as multiple toroidal and elliptical Alfvén eigenmodes (TAEs and EAEs) respectively, excited by ICRF-driven ^{4}He ions. Energetic ions can destabilise Alfvén eigenmodes, with the drive being proportional to the radial pressure gradient of the energetic ions, if the product of the toroidal mode number and ion diamagnetic frequency exceeds the mode frequency [14]. The ion diamagnetic frequency is proportional to the radial gradient of the distribution of energetic ions and increases with the tail temperature. Using the 70keV beams and identical ICRF power, no AEs were observed due to a radial distribution of ions with lower energy.

Moreover, as expected in the presence of centrally peaked high-energy particles [3,5], the electron temperature T_e represented in Figure 1 shows a more stabilised sawtooth activity in discharge with 120keV beams. The increase in sawtooth period with a higher fast ion energy W_{fast} (W_{fast} in the case of 120keV 4He beams has been estimated as up to 40% larger than when using 70keV ^{4}He beams) appears to be consistent with the stabilising effect of the fast ^{4}He on the $1 = m$ $1 = n$ internal kink mode [15]. Indeed, the increase in W_{fast} is mainly near the plasma centre, where the ^{4}He 3rd harmonic cyclotron resonance is located, i.e. inside the rational surface $q = m/n = 1$ located around $r/a \approx 0.5$ (where q is the tokamak safety factor defined as $q \approx rB_T/RB_p$ with r the plasma minor radius, B_T the toroidal field, B_p the poloidal field).

Finally, as illustrated on Figure 4, the crashes of sawteeth with long periods trigger magnetic perturbations with toroidal and poloidal numbers equal to $n = 2$, $m = 3$ or $n = 3$, $m = 4$ which have been identified as NTMs. This observation confirms the relationship between crashes of strongly stabilised sawteeth and NTMs 19. The long sawtooth crashes together with the NTMs led to degradation of the plasma performance as observed on the plasma diamagnetic energy. In the next section, we will focus on the sawteeth and NTM control.

3. SAWTOOTH ACTIVITY CONTROL RELEVANT FOR BURNING PLASMAS

Sawtooth stabilisation by a-particles in a reactor can have deleterious effects e.g. by triggering plasma instabilities such as NTMs at normalised plasma pressure β_N values much lower than the ideal MHD limit [16,17,18] (an example is shown in Figure 4). These modes form islands near resonant magnetic surfaces, at q = 3/2 and 2/1 in particular, and their main detrimental effects are a loss of energy and particle confinement which could adversely affect the performance in scenarios foreseen in ITER. It is known that a finite seed island width is required to lead to NTM destabilisation [18] and that this critical width is often triggered at the crash of a long sawtooth [19. 25]. On the other

hand, sawtooth activity is deemed useful in a reactor to avoid ash accumulation in the centre. Therefore, a new scenario [19, 20] based on the use of ICRF waves, has been developed at JET in which the sawtooth activity is maintained but at such a level that the NTM induced seed islands are small.

ICRF waves can be used to affect the sawteeth activity in two ways. The first is sawtooth stabilisation due to a high fast-ion pressure in the plasma core when the minority ion cyclotron resonance layer is located near the plasma centre [3, 4, 5]. The second is a sawtooth stabilisation or destabilisation due to a local modification of the magnetic shear $s = (r/q)(dq/dr)$ near $q = 1$ in response to the current driven by fast ions [21, 22]. The method of driving current by heating minority ions with toroidally directed waves (i.e. with an average finite wave number // k in the direction parallel to the magnetic field) at a frequency $f = \omega/(2\pi)$ equal to the minority ion cyclotron frequency $f_{c_i} = \omega_{c_i}/(2\pi)$ was originally proposed by Fisch [21] and is based on the Doppler shift of the cyclotron resonance, $\omega - n_{harmonic}\,\omega_{c_i} - k_{||}\,v_{||} = 0$. This shift leads to an asymmetrical interaction of ICRF waves with ions and electrons. Depending of the resonance position, the current produced is expected to locally modify the shear leading to sawteeth stabilisation or destabilisation.

A comparison of ICRF waves effect on sawteeth with -90^{o} phasing (corresponding to asymmetric waves with $k_{||} < 0$ i.e. counter-current) and $+90^{o}$ phasing (corresponding to asymmetric waves with $k_{||} > 0$ i.e. co-current), is shown on Figure 5. By working with an ICRF wave frequency of 42MHz and by ramping the magnetic field B between 2.2T and 3T the first harmonic H minority ion cyclotron resonance layer $H_{res}(H)$, was moved from 2.4m (plasma inner side) to 3.0m (plasma centre), crossing the sawtooth inversion radius R_{INV} located at around 2.7m. Up to 5MW of ICRF power, P_{ICRF}, was applied with an H minority concentration in D estimated to 5%. With -90^{o} phasing and $R_{res}(H)$ positioned close to R_{INV}, the sawtooth period and amplitude were dramatically reduced and the sawteeth activity almost completely disappeared. On the contrary at the same relative position but with $+90^{o}$ phasing, sawteeth stabilisation was obtained. As the resonance was moved further towards the centre, the ICRF fast ion pressure inside $q = 1$ increased and became the dominant factor behind the sawtooth stabilisation. It has to be noted that due to the ICRF waves induced pinch in the presence of an asymmetric spectrum 23, a more peaked fast ion pressure was expected with $+90^{o}$ phased waves leading to a stronger sawtooth stabilisation, as observed.

In order to further demonstrate the effect of the ICRF waves on the sawtooth behaviour and also to find out the optimal ICRF power necessary for sawtooth destabilisation, another set of experiments, illustrated on Figure 6, were performed. In that case, the magnetic field was fixed in order to position $R_{res}(H)$ very close to R_{INV} or in the plasma centre and the ICRF power P_{ICRF} was ramped from 0 to 10MW. In the discharge 55829, with central H cyclotron resonance layer, sawtooth stabilisation was obtained. The sawtooth period increase was found consistent with the fast ion energy increase, as the ICRF power was ramp-up. For the pulse 55828, $+90^{o}$ phased waves were used and $R_{res}(H)$ was positioned close to R_{INV}. In that case, a significant sawtooth stabilisation was obtained from $t \approx 19s$ corresponding to P_{ICRF} $4MW$. In the same configuration but with a -90^{o} phasing (pulse 55827) the sawtooth periods was kept very short throughout the power ramp with an

optimal effect between $t = 18s$ and $t = 19s$ corresponding to P_{ICRF} between 4 and 6MW. Because of the very small sawtooth activity even at high ICRF power, the local modification of the shear around q = 1 by ICCD is expected to be the dominant effect in this pulse.

When required, this technique is now used regularly at JET in order to avoid monster sawteeth. It has to be noted that other similar scenarios have been developed using the ICRF waves tuned to the second harmonic H cyclotron resonance [24, 25, 26]. Experiments have also been performed in order to produce ICCD with toroidally symmetric wave spectra, which can still be achieved due to the finite orbit width and effects of non–standard orbits of trapped ions [24, 27, 28].

ICCD sawtooth control has also been applied in order to increase the N b threshold at which NTMs are triggered [19]. An example is given on Figure 7, with two discharges for which only the ICRF phasing differs and with the resonance position located near the sawtooth inversion radius. One can see that for the discharges using -90^{o} phasing, in which the sawtooth activity is destabilised, larger bN value was obtained without triggering NTMs.

Finally another scenario has recently been developed to study the capabilities of ICCD to destabilise monster sawteeth created by fast ions like a-particles in burning plasmas. In these experiments [29], two of the four JET A2 ICRF antennas were tuned to a frequency corresponding to $R_{res}\ (H)$ in the plasma centre with a $+90^{o}$ phasing in order to maximise the central fast ion pressure and the other two tuned to a frequency corresponding to $R_{res}\ (H)$ on the sawtooth inversion radius and with a -90^{o} phasing. Successful ICRF sawtooth destabilisation of long sawtooth generated by ICRF-driven fast ions has been obtained. In the future, this "two frequency" scenario could be applied, to the experiments described in paragraph I in order to control sawteeth and NTMs created by the fast 4He ions.

4. SIMULATED ALPHA PARTICLE SELF-HEATING EXPERIMENTS

In JET D-only plasma the a-particle power is zero and in JET-DT plasma 30, the maximum fraction of α-heating f_{α} obtained was about 12% (Q ~ 0.65). Therefore to study at JET the evolution of a P_{α} in ITER-type plasma, the heating effects of a-particles have to be simulated using the available heating system. In this set of experiments [31, 32], the dynamic of α-particles heating and control of an equivalent $Q = 10$ burn was experimentally investigated using D plasma and ICRF heating. In order to obtain mainly electron heating with a central deposition as expected for an a-particles self-heated plasma, ICRF waves with a frequency of 37MHz corresponding to the first harmonic H minority ions cyclotron resonance in the plasma centre, were used. Using the JET Real-Time Central Control (RTCC) network, one component of the ICRF heating was applied in response to real-time measured plasma parameters such as neutron rate, density and plasma temperature to simulate the self-heating effect from α- particles $P_{\alpha,sim}$, a and a second component was used as external heating P_{ext} to control the "burn".

One of the main aims of these experiments was to demonstrate the qualitative features and to control a situation of "thermal runaway". Indeed, from simple power balance considerations [33],

three distinct operating regimes may be identified, depending of the value of Q. For $0 < Q < Q_{runaway}$, the plasma is unconditionally stable. For $Q > Q_{runaway}$ a change in plasma energy W results in a change of P_α (or $P_{\alpha,sim}$) greater than the increase of the loss power P_{loss}. In this second regime, referred to the thermal runaway regime, the a-power is expected to be subject to an unstable excursion but P_{ext} can be reduced to compensate, thus feedback control of the a-power via *ext P* should be possible. In the third regime, the plasma is fully ignited, the a-power exceeds the losses and $P_{ext} = 0$, so burn control other than P_{ext} mechanism would be required.

In order to have a similar plasma regime and configuration as that foreseen for a reactor, the experiments were performed in ELMy-H mode in a divertor configuration, with a magnetic field B of 2.5T and a plasma current I_p of 2.5MA. A qualitatively "reactor similar" trajectory in terms of P_{ext} and density ramp-up was programmed. The power level and density were chosen to ensure an L to H mode transition occurring towards the end of the P_{ext} ramp. Two experimental scenarios were investigated with two different feedback controls for $P_{\alpha,sim}$. In the first set of experiments, $P_{\alpha,sim}$ was evaluated as proportional to the changes of the DD reaction rate $P_{\alpha,sim}(t) = C_\alpha \Delta R_{DD}(t)$ Indeed, it was found that the DD reaction rate variation ΔR_{DD} was proportional to $T_e(0)^{1.5\text{-}2.0}$ where $T_e(0)$ is the central electron temperature) in a similar way that the appropriate scaling of the thermal DT reaction rate R_{DT}. The value of the coefficient C_α was determined using the value of R_{DT} at a maximum ICRF power of 10MW and in order to have $Q \approx 10$ i.e. $P_{\alpha,sim} \approx 6.6MW$, and $P_{ext} \approx 3.3MW$. The first results, obtained with the P_{ext} component of ICRF power simply pre-programmed, are presented in Figure 8, showing the evidence of onset of thermal runaway for $8 \gg Q$; during this phase $dP_{\alpha,sim}/dt > dP_{loss}$, a , until $t = 20.5$s when the P_{ext} component was deliberately reduced. For a plasma of stored thermal energy W , it may be shown [33], that as $P_{\alpha,sim} \propto W^{\Psi}$ and $\tau_E \propto P_{\alpha,sim}^{\nu}$, the necessary condition for a thermal runaway onset is $Q > Q_{rumaway} = 5/(\Psi + \Psi\upsilon - 1)$ Assuming $\Psi \approx 2$ (reference value for a ITER-like plasma) implies that during the steady conditions of the early H-mode phase in Figure 8, $\upsilon \approx -0.2$ u which corresponds to a rather weak degradation of confinement with loss power (most scaling laws have υ between –0.5 and –1). During the later phase of the H-mode however $P_{\alpha,sim}$ remained constant or declined slightly, implying a stronger degradation of the confinement with the power losses. For the discharges represented on Figure 9, a feedback term was added to the pre-programmed P_{ext} waveform in order to stabilise $P_{\alpha,sim}$ at a reference level. This level was stepped up around $t = 25s$ in order to observe the overall system response. Note also the strong variation in $P_{\alpha,sim}$, a due to sawteeth and the partially compensating effect of P_{ext}.

In the second set of experiments the algorithm for calculating $P_{\alpha,sim}$ was based on a parametrised fit to the volume-integral of thermal DT reaction rate R_{DT} (for a 50:50 D:T mix assuming that the electron and ion temperatures are equal and a flat density profile): $P_{\alpha,sim}(t) = C_\alpha . R_{DT,sim}(t)$ and $R_{DT,sim} = n_e(0)^2 . F(S_T T_e(0),\ T_e(0)/\langle T_e \rangle)$ where $T_e(0)$ is the central electron temperature, $\langle T_e \rangle$ is the volume averaged electron temperature, $n_e(0)$ is the central electron density, $S_T = 3$ represents the electron temperature scale factor between ITER and JET, and F is the parameterised fit function. C_α was again chosen to obtain $Q \approx 10$ at maximum ICRF power. The imput parameters $T_e(0)$, $\langle T_e \rangle$,

$n_e(0)$ were available in real-time via the JET RTCC network from the electron cyclotron emission and interferometers measurements respectively. Figure 10 gives results of a discharge using this second scenario and shows similar behaviour than the discharges in Figure 8 and Figure 9 except that the thermal instability is more pronounced, reflecting the more realistic calculation of $P_{\alpha,sim}$. In the same way as for discharge 52608, represented in Figure 9, the P_{ext} component of the ICRF heating was controlled under feedback from $s\ t\ 20 =$ and the excursion of $P_{\alpha,sim}$ was satisfactory stabilised.

It should be noted that there are fundamental limitations to these kinds of scale-model experiments of reactor-like scenarios. Indeed, it is not possible to preserve all the relevant dimensionless time-scales. For example, in the discharges represented on Figure 9, PION 34 code simulations showed that, as expected, 90% of the ICRF power was delivered to the electrons and that the fast ion H minority energy contributed to around 30% of the total plasma energy, with a ratio of the thermal energy confinement time to the fast ion slowing down time $\tau_S/\tau_e \approx 0.4$. This compares with value of around 7% and 0.04 respectively for unthermalised a-particles in the $Q = 10$ ITER reference scenario. This kind of discrepancy can be expected to affect the dynamic behaviour of, otherwise similar, discharges and hence the reliability of the simulation. Nevertheless, even if it is not possible to satisfy all the required similarity conditions, several of the expected dynamic features of self-heated plasmas have been demonstrated.

SUMMARY

Experiments have been carried out on the JET tokamak in order to investigate further burning plasma physics. In ^{4}He plasmas, ICRF power at the third harmonic ^{4}He ion cyclotron resonance has been added to ^{4}He NBI ions in order to explore for the first time plasmas with significant heating by fast ^{4}He. ^{4}He with energies above 2MeV has been observed by the γ-ray emission diagnostic demonstrating the feasibility of the reaction ^{9}Be(α, n γ)^{12}C for burning plasmas. Both TAEs and EAEs have been excited by the fast ^{4}He produced but no adverse effect on the plasma confinement has been observed. Sawtooth stabilisation has been obtained as well as NTMs onset at crashes associated with long sawtooth periods.

The use of ICRF toroidally directed waves has been investigated as a tool to control the sawtooth activity. Successful sawtooth destabilisation has been obtained by using -90^o phased waves with the H cyclotron resonance layer positioned near the sawtooth inversion radius. This technique has been applied in order to increase the plasma pressure at which NTMs are triggered.

Thermal instability in an experimental simulation of a-particles self-heated plasma with predominant electron heating in deuterium discharges has been demonstrated. The thermal excursion has been successfully stabilised by feedback control on the external power.

ACKNOWLEDGEMENTS

Is it a pleasure to thank our colleagues at JET who operates the tokamaks, the heating systems and the diagnostics during experiments. The work carried out by the UKAEA personnel was jointly funded by the United Kingdom Engineering and Physical Sciences Research Council and by EURATOM.

REFERENCES

[1]. ITER Physics Basis Editors, ITER Physics Expert Group Chairs and Co-Chairs and ITER Joint Central Team and Physics Integration Unit , Nuclear Fusion **39**, 12 (1999)

[2]. A.S. Fasoli *et al.*, Plasma Phys. Control. Fusion **39,** B287 (1997).

[3]. F. Porcelli, Plasma Phys. Controlled Fusion **33**, 1601-1620 (1991).

[4]. F. Porcelli *et al*., Plasma Phys. Control Fusion **38**, 2163 (1996).

[5]. D.J. Campbell *et al*., Phys. Rev. Lett. **60** (1988).

[6]. J. Candy *et al.*, Proceedings of 24th European Physical Conference, Brechtesgaden, 1997, ECA Vol. 21A, Part III, 1189 (1997).

[7]. M.J. Mantsinen *et al.*, Phys. Rev. Lett. **88**(10), 105002-1, (2002).

[9]. V.G. Kiptily *et al*., Nucl. Fusion **42**, 999 (2002).

[9]. A.A. Korotkov, A. Gondhalekar, and R.J. Akers, Phys. Plasmas, **7**, 957 (2000).

[10]. D.F. Start *et al.*, Nucl. Fusion **39(3)**, 321 (1999).

[11]. L.-G. Eriksson *et al.,* Phys. Rev. Lett. **81**, 1231 (1998).

[12]. A. Fasoli *et al.,* Plasma Phys. Controlled Fusion **33**, 1601 (1991).

[13]. R. Heeter *et al*., Proceedings of the 5th IAEA Technical Committee Meeting on Alpha Particles in Fusion Research, JET, United Kingdom, 1997 (JET, Abingdon, UK, 1997).

[14]. W. Kerner *et al.*, Nucl. Fusion **38** 1315 (1998).

[15]. F. Porcelli, Plasma Phys. Controlled Fusion **33**, 1601 (1991)

[16]. O. Sauter, *et al.* , Phys. Plasmas **4**, 1654-1664 (1997).

[17]. R.J. La Haye, O. Sauter, Nucl. Fusion **38**, 987-999 (1998).

[18]. R. Buttery, *et al*, Plasma Phys. and Controll. Fusion, **42** B61-B73 (2000).

[19]. O. Sauter et al., Phys. Rev. Lett.**88**(10), 105001-1 (2002).

[20]. M.-L. Mayoral *et al.*, Proceedings of 14thTopical Conference RF Power in Plasmas,Oxnard, 2001, AIP Vol.595, 106 (2001).

[21]. N.J. Fish, Nucl. Fusion **21**, 15(1981.)

[22]. V.P. Bhatnagar, *et al*., Nucl. Fusion **34**, 1579-1603 (1994).

[23]. L.-G. Eriksson, *et al.*, Phys. Rev. Lett. **81(6)** (1998) 1231

[24]. M. J. Mantsinen, *et al*., Plasma Phys. Contr. Fusion **44**,1521 (2002)

[25]. E. Westerhof*, et al*., Nucl. Fusion 42 1324 (2002).

[26]. M.-L. Mayoral *et al.*, Proceedings of 27thEuropean Physical Conference Montreux, 2002, ECA Vol. 26B (2002).

[27]. J. Carlsson, *et al.,* Phys. Plasmas **5**, 2885 (1998)

[28]. T. Hellsten *et al*., Phys. Rev. Lett. **74,** 3612 (1995).

[29]. L.-G. Eriksson *et al* to be submitted to Phys. Rev. Lett.

[30]. M. Keilhacker *et al.,* Nucl. Fusion 39(2), 209 (1999)

[31]. T.T.C Jones *et al.* , Proceedings of 28th European Physical Conference Funchal, 2001, ECA Vol. 25A, 1197 (2001).

[32]. J.-M. Noterdaeme *et al.*, Nucl. Fusion **43**, 202 (2003)

[33]. N.H. Zornig, PhD thesis, Brunel University, United Kingdom (1998).

[34]. L.-G. Eriksson, T. Hellsten, and U. Willen, Nuclear Fusion **33**, 1037 (1997)

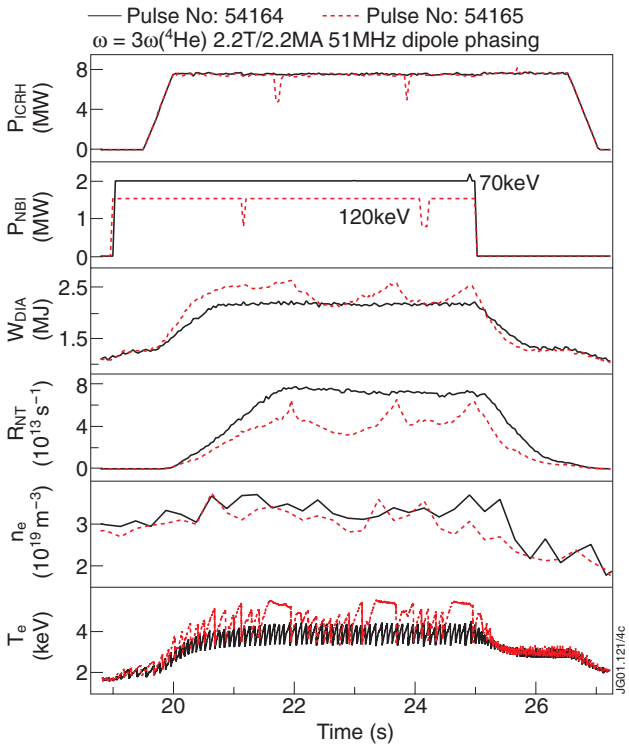

Figure 1: Overview of Pulse No's: 54164 and 54165, with heating at the ^{4}He 3rd harmonic cyclotron resonance combined with 70keV and 120keV ^{4}He beams, respectively.

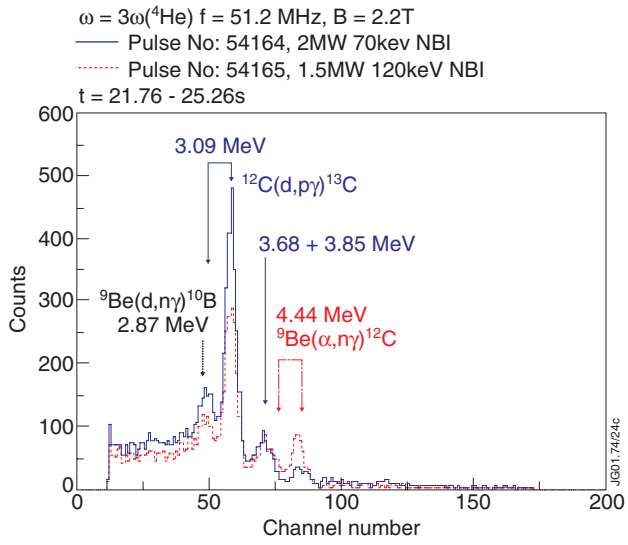

Figure2: Gamma ray spectra for the two discharges in Fig.1.

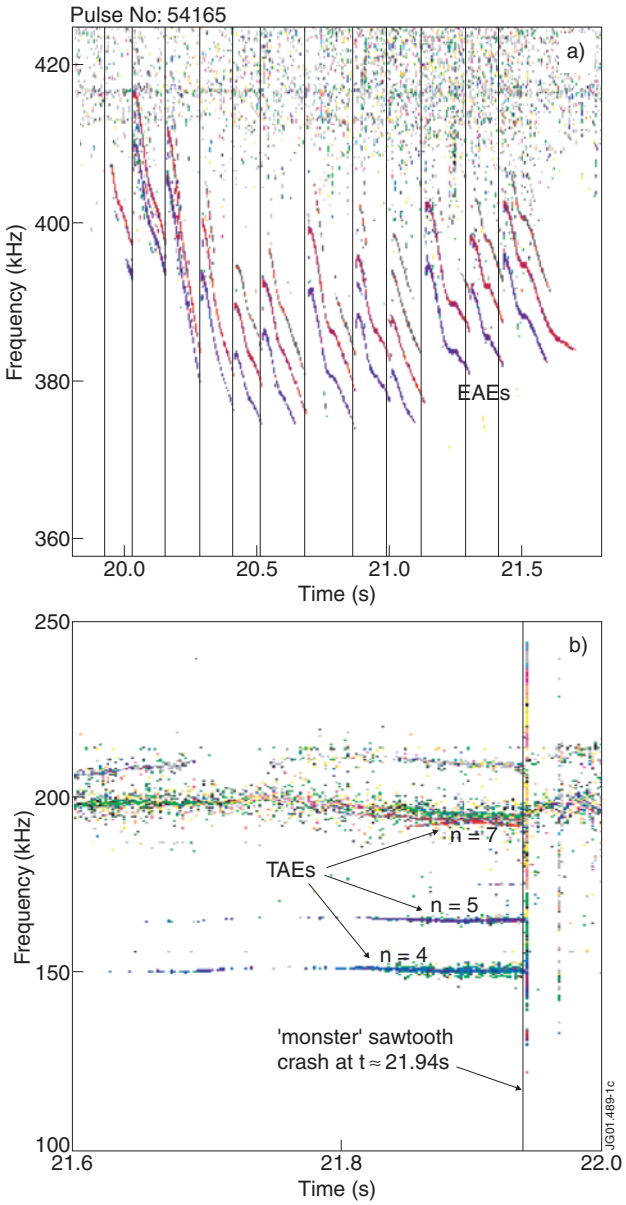

Figure 3: Magnetic fluctuation spectrograms showing (a) elliptical and (b) toroidal Alfvén eigenmodes. The vertical lines indicate the sawtooth crashes.

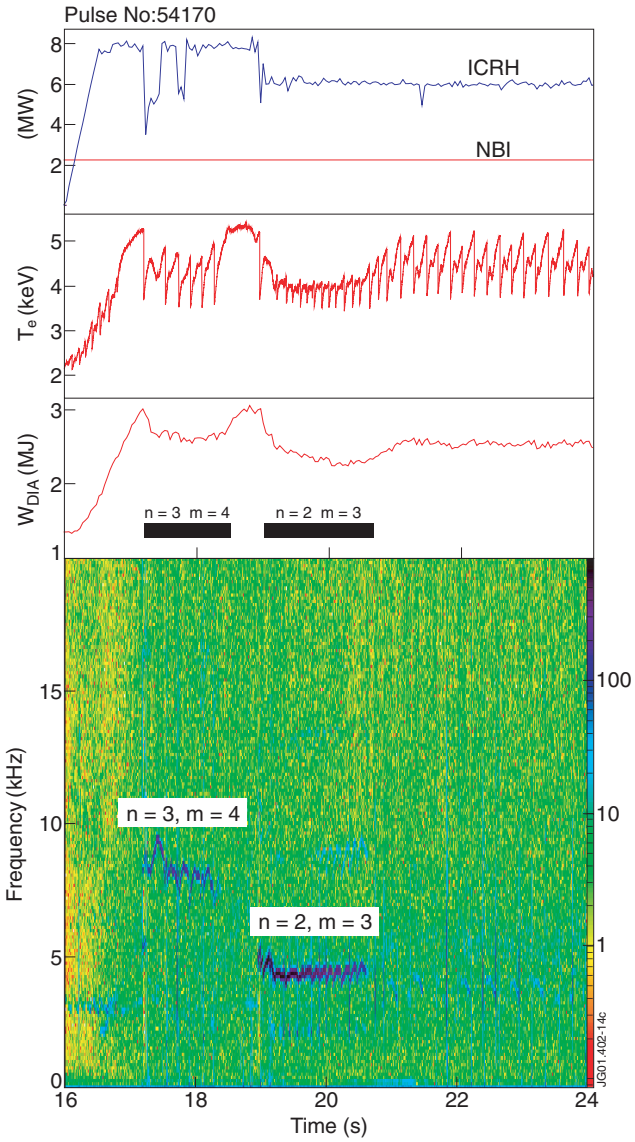

Figure 4: Overview of the Pulse No: 54170 with $\omega \approx 3\omega_c$ (^{4}He) and 120keV beams. The magnetic fluctuation spectrogram shows magnetic perturbations triggered by the sawtooth crashes in the Pulse No: 54170.

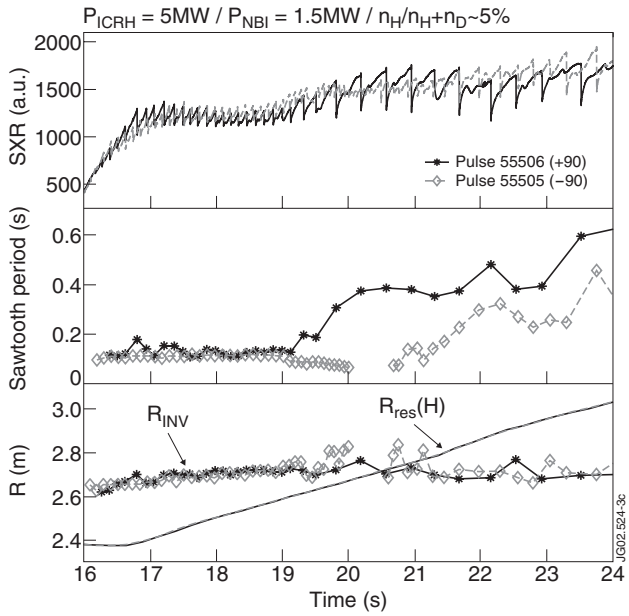

Figure 5: Soft x-ray emission, sawtooth period, sawtooth inversion radius R_{inv} and H minority resonance layer $R_{res}(H)$ for the Pulse No's: 55506 ($+90^o$ phasing), 55505 (-90^o phasing).

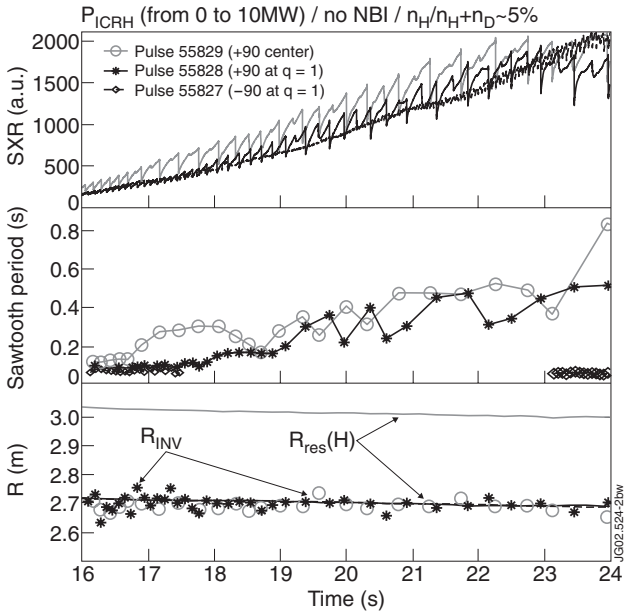

Figure 6: Soft x-ray emission (central channel), sawtooth period, sawtooth inversion radius R_{inv} and H minority cyclotron resonance layer $R_{res}(H)$ for the discharges 55829 ($+90^o$ phasing and $R_{res}(H)$ in the centre), 55828 ($+90^o$ phasing and $R_{res}(H)$ on R_{inv}, 55827 (-90^o phasing and $R_{res}(H)$ on R_{inv}). In Pulse No: 55827, the sawtooth activity is kept low trough the ICRF power ramp-up.

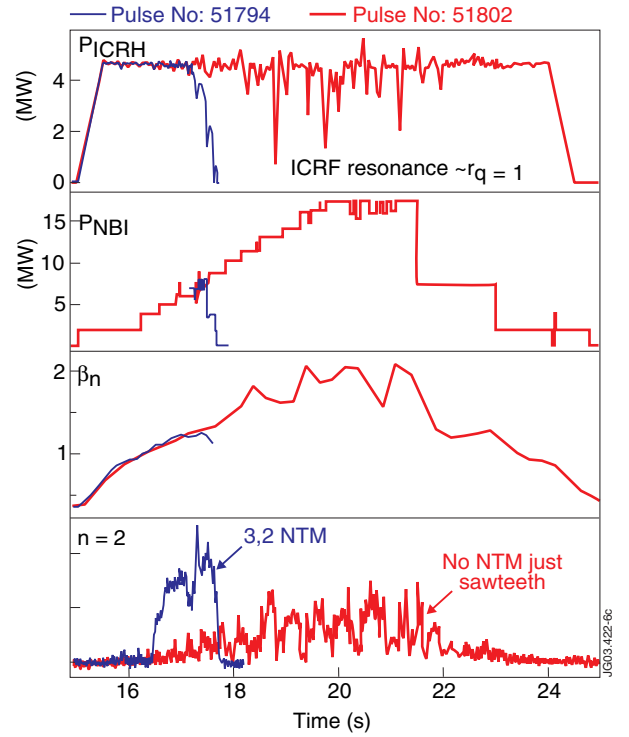

Figure 7: Comparison of two discharges with ICCD applied with the resonance close to the sawtooth inversion radius. In discharge with -90^o phasing (Pulse No: 51794), larger β_N value is obtained without triggering NTMs [19].

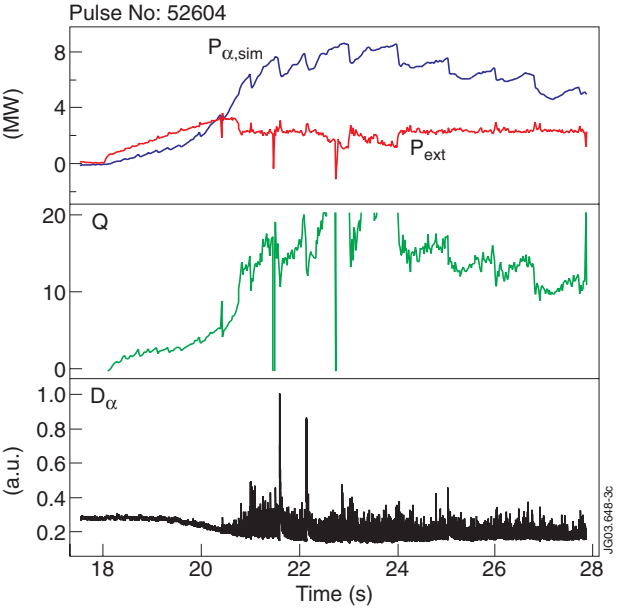

Figure 8: ICRF power in roles of P_{ext} and $P_{\alpha,sim}$, fusion gain factor $Q = 5P_{\alpha,sim} / P_{ext}$ and ELMs behaviour for Pulse No: 52064.

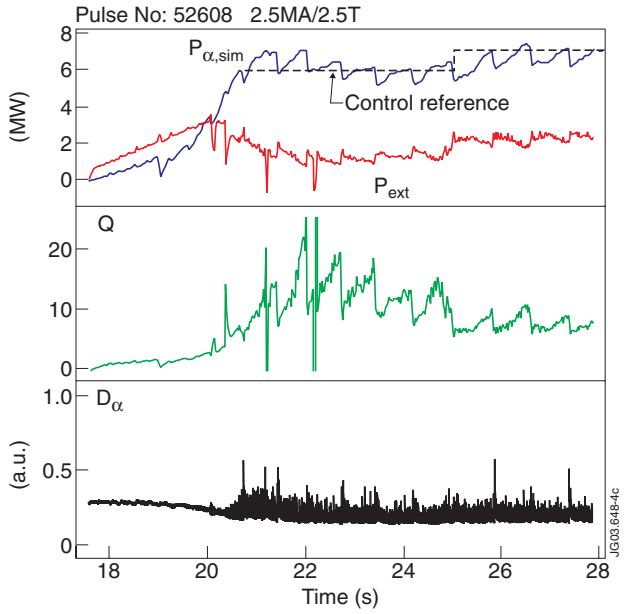

Figure 9: ICRF power in roles of P_{ext} and $P_{\alpha,sim}$, fusion gain factor $q = 5P_{\alpha,sim}/P_{ext}$ and ELMs behaviour for pulse 52608. Step-change increase in $P_{\alpha,sim}$ demand achieved via feedback control on P_{ext}.

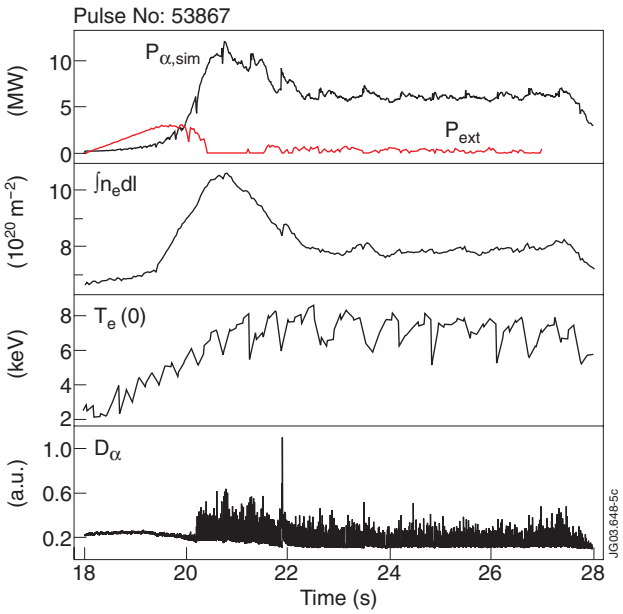

Figure 10: ICRF power in roles of P_{ext} and $P_{\alpha,sim}$, line integrated electron density, central electron temperature and ELMs behaviour for Pulse No: 53867. $P_{\alpha,sim}$ scaled from parameterised fit to DT reaction rate in equivalent DT plasma using the electron temperature and density as input.